

# Combretastatin A-4 and Derivatives: Potential Fungicides Targeting Fungal Tubulin

Zhong-lin Ma,<sup>†</sup> Xiao-jing Yan,<sup>§</sup> Lei Zhao,<sup>†</sup> Jiu-jiu Zhou,<sup>†</sup> Wan Pang,<sup>†</sup> Zhen-peng Kai,<sup>\*,†</sup> and Fan-hong Wu<sup>\*,†,#</sup>

<sup>†</sup>School of Chemical and Environmental Engineering, Shanghai Institute of Technology, Shanghai 201418, People's Republic of China

<sup>§</sup>Institute of Plant Protection, China Academy of Agricultural Sciences, Beijing 100193, People's Republic of China

<sup>#</sup>Shanghai Engineering Research Center of Pharmaceutical Progress, Shanghai 201203, People's Republic of China

**ABSTRACT:** Combretastatin A-4, first isolated from the African willow tree *Combretum caffrum*, is a tubulin polymerization inhibitor in medicine. It was first postulated as a potential fungicide targeting fungal tubulin for plant disease control in this study. Combretastatin A-4 and its derivatives were synthesized and tested against *Rhizoctonia solani* and *Pyricularia oryzae*. Several compounds have EC<sub>50</sub> values similar to or better than that of isoprothiolane, which is widely used for rice disease control. Structure–activity relationship study indicated the the *cis* configuration and hydroxyl group in combretastatin A-4 are crucial to the antifungal effect. Molecular modeling indicated the binding sites of combretastatin A-4 and carbendazim on fungal tubulin are totally different. The bioactivity of combretastatin A-4 and its derivatives against carbendazim-resistant strains was demonstrated in this study. The results provide a new approach for fungicide discovery and fungicide resistance management.

**KEYWORDS:** *combretastatin, fungicide, resistance, tubulin, molecular modeling*

## ■ INTRODUCTION

Fungi can cause serious crop diseases, resulting in critical losses of yield and quality. Use of resistant varieties, biological control, and chemical fungicides are the common strategies for managing crop diseases. At present, chemical treatment with fungicides is the most common method to control those diseases. However, fungicide resistance has been detected in many fungal species and causes unsatisfactory control efficacy. It is necessary to develop new fungicides that have new structures and new antifungal mechanisms to address this problem.

Combretastatin A-4, which was first isolated from the African willow tree *Combretum caffrum*,<sup>1</sup> was identified as an attractive lead compound for the development of novel anticancer agents that utilize starvation tactics to attack widespread necrosis of solid tumors, including multidrug-resistant ones. It exerts a potent inhibition of tubulin polymerization by binding to the colchicine site and, as a consequence, demonstrates strong suppressive activity on tumor blood flow (TBF).<sup>2–4</sup>

Microtubules are biopolymers that are composed of self-associating  $\alpha$ - and  $\beta$ -tubulin heterodimers. Because they play an important role in a number of cellular processes, including maintaining the structure of the cell, cell movement, intracellular transportation, and cell division, microtubules are attractive targets for drug and pesticide design.<sup>5</sup> Carbendazim and other benzimidazole fungicides, well-known  $\beta$ -tubulin interferers, have been widely used to control various plant diseases for decades in China and in many other parts of the world. However, these fungicides have generally lost their efficacy because of the resistance after being used for 2 or 3 years.<sup>6</sup> Resistance to benzimidazole fungicides usually resulted from certain point mutations in the target  $\beta$ -tubulin gene.<sup>7</sup>

As combretastatin A-4 is a tubulin polymerization inhibitor in medicine, we postulated it also has an effect on the fungal

tubulin. Herein we report the syntheses of combretastatin A-4 and its derivatives via the Wittig reaction and the evaluation of their in vitro antifungal bioactivities. Molecular modeling was performed to determine the binding site of combretastatin A-4. The potential use of combretastatin A-4 and its derivatives for fungal resistance management was also evaluated in this study.

## ■ MATERIALS AND METHODS

**General Experimental Procedures.** All of the chemicals and reagents were commercially available and required no further purifications. Solvents were dried and freshly distilled before use according to literature procedures. Isoprothiolane (98% purity) was purchased from Lianyungang Liben Agro-chemical Co., Ltd. (Liangyungang, China). Carbendazim (98% purity) was purchased from Zhejiang Yifan Chemical Industry Co., Ltd. (Wenzhou, China). Melting points were determined using a WRS-2A melting point apparatus (Shanghai ShenGuang Instrument Co., Ltd., Shanghai, China). TLC analyses were performed on precoated silica gel polyester plates (Yantai Jiang You Silicone Development Co., Ltd., Yantai, China) with a fluorescent indicator UV 254. Chromatographic separations were performed on silica gel flash columns. <sup>1</sup>H NMR and <sup>13</sup>C NMR spectra were recorded on an AVANCE III at 500 MHz or on an Avance DMX500 spectrometer (Bruker, Fällanden, Switzerland) at 101 Hz in chloroform-*d* using TMS ( $\delta$  0.0 ppm) as an internal standard. IR was recorded on a 6700 FT-IR (Nicolet, Madison, WI, USA). HRMS were recorded on a solariX 70 FT-MS spectrometer (Bruker) using methanol/water (1:1, v/v) as solvent. LC-mass spectra were recorded on an LCMS-2020 spectrometer from Shimadzu Corp. (Kyoto, Japan) with acetonitrile and water as the mobile phase, and the gradient was from 5% acetonitrile at 0 min to 100% acetonitrile at 10 min. The column used

**Received:** October 25, 2015

**Revised:** December 28, 2015

**Accepted:** December 29, 2015

**Published:** December 29, 2015

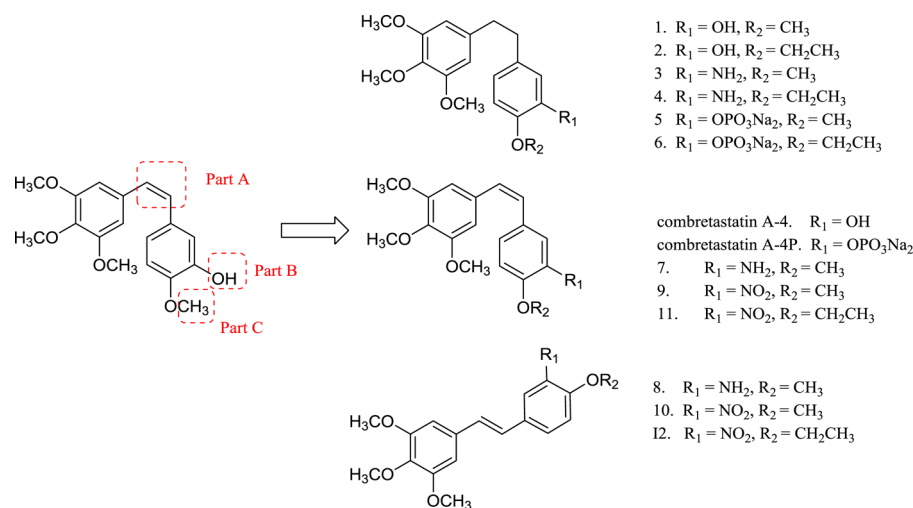


Figure 1. Chemical structures of combretastatin A-4 and derivatives.

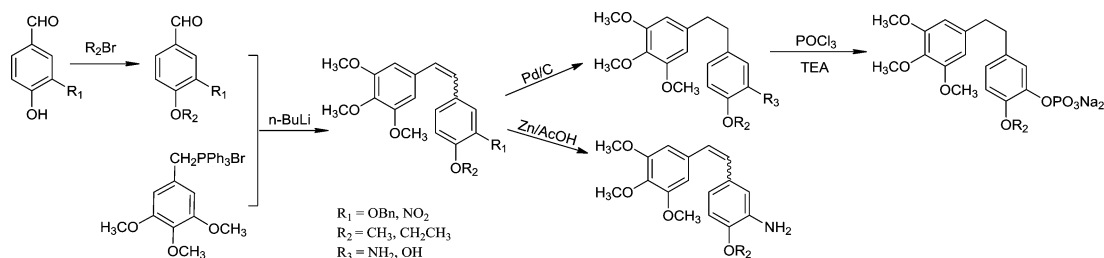


Figure 2. Synthesis of combretastatin A-4 derivatives.

was a 150 mm  $\times$  4.6 mm i.d., 5  $\mu\text{m}$ , Gemini RP-18 (Phenomenex, Torrance, CA, USA).

(*Z*)-2-Methoxy-5-(3,4,5-trimethoxystyryl)phenol (combretastatin A-4) and (*Z*)-2-methoxy-5-(3,4,5-trimethoxystyryl)phenyl disodium phosphate (combretastatin A-4P) were synthesized following the methods of Shen et al.<sup>8</sup> and Pettit et al.<sup>1</sup> Combretastatin A-4 derivatives were synthesized with the methods previously reported.<sup>9</sup>

**Bioassays.** Antifungal effects of compounds against *Rhizoctonia solani* Kühn (rice sheath blight disease), *Pyricularia oryzae* Cav (rice blast disease), and carbendazim-resistant strains *Fusarium oxysporum* Schl. f. sp. *vasinfectum* (Atk.) Snyder & Hans (cotton Fusarium wilt) and *Sclerotinia sclerotiorum* (Lib.) de Bary (rape Sclerotinia rot) were evaluated using mycelium growth rate test. All fungal strains were provided by the Institute of Plant Protection, Chinese Academy of Agricultural Sciences. Carbendazim was dissolved in 0.1 M HCl at 10 mg/mL as a stock solution and was added to autoclaved potato sucrose agar (PSA) that had been cooled to 45–50 °C. The pH value was adjusted with HCl to 6.8 in all media. Isoprothiolane, combretastatin A-4, and derivatives were dissolved in dimethyl sulfoxide (DMSO) and then mixed with the autoclaved PSA. A mycelial plug (7 mm in diameter) taken from the edge of a 4-day-old colony of strains was grown in the dark for 3 days at 25 °C in a 9 cm diameter Petri plate containing PSA amended with different concentrations of fungicides. The radial growth from the edge of the plug to the edge of the colony of each strain was measured after 3 days at 25 °C. For each plate, the average colony radial growth, measured in two perpendicular directions, was used for calculation of the inhibition. Data presented as percentages were log-transformed before statistical analyses. Data were analyzed using a one-way analysis of variance (ANOVA) with a Dunnett's multiple-comparison test as the post hoc determination of significance using GraphPad Prism version 5.0 (GraphPad Software, San Diego, CA, USA). Dose–response curves were also prepared using the computer program GraphPad Prism. Values are expressed as mean  $\pm$  standard errors (SE) with *n* indicating the number of samples measured (*n* = 3–5).

**Molecular Modeling.** The sequence of *R. solani*  $\beta$ -tubulin was retrieved from GenBank using a combination of BLAST and keyword searches. A crystal structure of cow brain  $\beta$ -tubulin (PDB ID 1Z2Bb) was used as the 3D coordinate template for the homology modeling. The homology model for *R. solani*  $\beta$ -tubulin was generated using FUGUE<sup>10</sup> and ORCHESTRAR module in Sybyl.<sup>11</sup> The initial model was optimized energetically using the minimize program with steepest descent algorithm, AMBER7 FF99 as the force field and Gasteiger–Huckel as the atomic point charges. The minimization was terminated when the RMS gradient convergence criterion of 0.05 kcal/(mol $\cdot$ Å) was reached.

Combretastatin A-4 and carbendazim were constructed using the 2D sketcher module in Sybyl. Minimum energy conformations of all structures were calculated using the Minimize module of Sybyl. The force field was MMFF94 with an 8 Å cutoff for nonbonded interactions, and the atomic point charges were also calculated with MMFF94.<sup>12</sup> Minimizations were achieved using the steepest descent method for the first 100 steps, followed by the Broyden–Fletcher–Goldfarb–Shanno (BFGS)<sup>13</sup> method until the root-mean-square (RMS) of the gradient became <0.005 kcal/(mol $\cdot$ Å).<sup>14</sup>

The Surflex-Dock<sup>15</sup> module implemented in the Sybyl program was used for the docking studies. Each inhibitor was docked into the corresponding protein's binding site by an empirical scoring function and a patented search engine in Surflex-Dock, applied with the automatic docking. Other parameters were established by default in the software.

## RESULTS AND DISCUSSION

**Chemistry.** (*Z*)-2-Methoxy-5-(3,4,5-trimethoxystyryl)phenol (combretastatin A-4) and (*Z*)-2-methoxy-5-(3,4,5-trimethoxystyryl)phenyl disodium phosphate (combretastatin A-4P) were synthesized following previously reported methods.<sup>1,7</sup>

The double bond in part A of combretastatin A-4 was hydrogenated, the hydroxyl group in part B was replaced by an amino or nitro or disodium phosphate group, and the methoxy

Table 1. Chemical Data of Combretastatin A-4 and Derivatives

| compound            | yield (%) | mp (°C)         | mol wt | MS result                      | <sup>1</sup> H NMR   | <sup>13</sup> C NMR   |
|---------------------|-----------|-----------------|--------|--------------------------------|--|---|
| combretastatin A-4  | 35        | 116.8–117.6     | 316.35 | (M + H) <sup>+</sup> 317.1399  | (CDCl <sub>3</sub> , 500 MHz): δ 3.69 (s, 6H, 2 × OCH <sub>3</sub> ), 3.84 (s, 3H, OCH <sub>3</sub> ), 3.85 (s, 3H, OCH <sub>3</sub> ), 5.58 (s, 1H, OH), 6.41 (d, 1H, J = 12.0 Hz, CH), 6.46 (d, 1H, J = 12.0 Hz, CH), 6.53 (s, 2H, 2 × CH), 6.73 (d, 1H, J = 8.5 Hz, CH), 6.79 (dd, 1H, J = 8.5 Hz, J = 2.0 Hz, CH), 6.92 (d, 1H, J = 2.0 Hz, CH)        | (CDCl <sub>3</sub> , 101 MHz): δ 152.8, 145.7, 145.2, 137.1, 132.7, 130.6, 129.4, 128.9, 121.1, 115.0, 110.3, 106.1, 60.8, 55.9                   |
| combretastatin A-4P | 80        | 238–242         | 440.29 | (M + H) <sup>+</sup> 441.0681  | (D <sub>2</sub> O, 500 MHz): δ 3.64 (s, 6H, 2 × OCH <sub>3</sub> ), 3.70 (s, 3H, OCH <sub>3</sub> ), 3.81 (s, 3H, OCH <sub>3</sub> ), 6.41 (d, 1H, J = 12.0 Hz, CH), 6.56 (s, 2H, 2 × CH), 6.62 (d, 1H, J = 12.0 Hz, CH), 6.73 (d, 1H, J = 8.5 Hz, CH), 6.80 (d, 1H, J = 8.5 Hz, CH), 7.39 (s, 1H, CH)   | (D <sub>2</sub> O, 101 MHz): δ 151.8, 148.9, 148.8, 142.9, 142.8, 135.4, 133.5, 130.0, 129.9, 128.3, 122.2, 121.0, 112.1, 106.2, 60.6, 55.7, 55.6 |
| 1                   | 91        | 76–77           | 318.36 | (M + H) <sup>+</sup> 319.1475  | (CDCl <sub>3</sub> , 500 MHz): δ 2.82 (s, 4H, 2 × CH <sub>2</sub> ), 3.83 (s, 9H, 3 × OCH <sub>3</sub> ), 3.87 (s, 3H, OCH <sub>3</sub> ), 5.61 (s, 1H, OH), 6.38 (s, 2H, 2 × CH), 6.64–6.66 (m, 1H, CH), 6.77 (d, 1H, J = 8.0 Hz, CH), 6.81 (d, 1H, J = 3.0 Hz, CH)   | (CDCl <sub>3</sub> , 101 MHz): δ 154.1, 139.4, 136.0, 120.7, 116.7, 112.8, 106.9, 61.1, 56.5, 56.4, 49.3, 49.2, 48.9, 48.8, 48.6, 39.4, 38.3      |
| 2                   | 92        | 69.3–69.6       | 332.39 | (M + H) <sup>+</sup> 333.1741  | (CDCl <sub>3</sub> , 500 MHz): δ 1.43 (t, 3H, J = 5.0 Hz, CH <sub>3</sub> ), 2.82 (s, 2H, 2 × CH <sub>2</sub> ), 3.83 (s, 9H, 3 × OCH <sub>3</sub> ), 4.09 (q, 2H, J = 5.0 Hz, CH <sub>2</sub> ), 6.38 (s, 2H, 2 × CH), 6.62 (d, 1H, J = 5.0 Hz, CH), 6.75 (d, 1H, J = 5.0 Hz, CH), 6.81 (s, 1H, CH)   | (CDCl <sub>3</sub> , 101 MHz): δ 153.0, 145.6, 144.0, 137.6, 136.2, 134.9, 119.7, 114.6, 111.5, 105.4, 64.6, 60.8, 56.0, 38.4, 37.3, 14.9         |
| 3                   | 90        | nd <sup>a</sup> | 317.38 | (M + Na) <sup>+</sup> 340.0638 | (CDCl <sub>3</sub> , 500 MHz): δ 1.58 (s, 2H, NH <sub>2</sub> ), 2.80 (s, 4H, 2 × CH <sub>2</sub> ), 3.84 (s, 12H, 4 × OCH <sub>3</sub> ), 6.39 (s, 2H, 2 × CH), 6.55 (d, 1H, J = 10.0 Hz, CH), 6.58 (d, 1H, J = 5.0 Hz, CH), 6.71 (d, 1H, J = 10.0 Hz, CH)  | nd  |
| 4                   | 90        | 82.9–83.4       | 331.41 | (M + Na) <sup>+</sup> 354.1691 | (CDCl <sub>3</sub> , 500 MHz): δ 1.42 (t, 3H, J = 5.0 Hz, CH <sub>3</sub> ), 2.75–2.83 (m, 4H, 2 × CH <sub>2</sub> ), 3.83 (s, 9H, 3 × OCH <sub>3</sub> ), 4.04 (q, 2H, J = 5.0 Hz, CH <sub>2</sub> ), 6.39 (s, 2H, 2 × CH), 6.51–6.53 (m, 1H, CH), 6.59 (d, 1H, J = 5.0 Hz, CH), 6.70 (d, 1H, J = 5.0 Hz, CH)   | (CDCl <sub>3</sub> , 101 MHz): δ 153.1, 146.7, 145.9, 137.6, 136.2, 135.2, 134.4, 128.1, 122.7, 119.7, 111.9, 64.3, 60.9, 56.1, 38.5, 37.2        |
| 5                   | 86        | 266–269         | 442.31 | (M + Na) <sup>+</sup> 465.0617 | (D <sub>2</sub> O, 500 MHz): δ 2.77 (d, 2H, J = 13.7 Hz, CH <sub>2</sub> ), 2.81 (d, 2H, J = 13.7 Hz, CH <sub>2</sub> ), 3.67 (s, 3H, OCH <sub>3</sub> ), 3.69 (s, 6H, 2 × OCH <sub>3</sub> ), 3.75 (s, 3H, OCH <sub>3</sub> ), 6.47 (s, 2H, 2 × CH), 6.77 (d, 1H, J = 8.4 Hz, CH), 6.79 (d, 1H, J = 8.4 Hz, CH), 7.27 (d, 1H, J = 2.0 Hz, CH)             | (D <sub>2</sub> O, 101 MHz): δ 152.3, 148.1, 148.0, 143.3, 139.5, 135.1, 134.7, 121.7, 120.3, 120.6, 112.9, 106.2, 61.0, 56.3, 56.1, 37.6, 36.7   |
| 6                   | 50        | 140.3–141.0     | 456.33 | (M + Na) <sup>+</sup> 479.0813 | (D <sub>2</sub> O, 500 MHz): δ 1.33 (t, 3H, J = 5.0 Hz, CH <sub>3</sub> ), 2.78–2.81 (m, 4H, 2 × CH <sub>2</sub> ), 3.67 (s, 3H, OCH <sub>3</sub> ), 3.74 (s, 6H, 2 × OCH <sub>3</sub> ), 4.04 (q, 2H, J = 5.0 Hz, CH <sub>2</sub> ), 6.54 (s, 2H, 2 × CH), 6.65 (d, 1H, J = 5.0 Hz, CH), 6.84 (d, 1H, J = 10.0 Hz, CH), 7.38 (s, 1H, CH)                  | (D <sub>2</sub> O, 101 MHz): δ 152.1, 146.7, 143.7, 139.0, 135.1, 134.7, 121.7, 120.3, 114.2, 105.9, 65.4, 60.7, 55.8, 48.9, 37.4, 36.5, 14.1     |
| 7                   | 73        | nd              | 315.36 | (M + H) <sup>+</sup> 316.1555  | (CDCl <sub>3</sub> , 500 MHz): δ 3.70 (s, 6H, 2 × OCH <sub>3</sub> ), 3.83 (s, 3H, OCH <sub>3</sub> ), 3.84 (s, 3H, OCH <sub>3</sub> ), 6.37 (d, 1H, J = 12.0 Hz, CH), 6.46 (d, 1H, J = 12.0 Hz, CH), 6.55 (s, 2H, 2 × CH), 6.68 (s, 2H, 2 × CH), 6.70 (d, 1H, J = 1.0 Hz, CH)   | (CDCl <sub>3</sub> , 75 MHz): δ 152.8, 146.6, 137.0, 135.7, 132.9, 130.0, 128.4, 119.5, 115.2, 110.1, 106.0, 60.9, 55.9, 55.5                     |
| 8                   | 85        | 110–112         | 315.36 | (M + H) <sup>+</sup> 316.1555  | (CDCl <sub>3</sub> , 500 MHz): δ 3.65 (s, 3H, OCH <sub>3</sub> ), 3.76 (s, 3H, OCH <sub>3</sub> ), 3.81 (s, 6H, 2 × OCH <sub>3</sub> ), 4.74 (s, 2H, NH <sub>2</sub> ), 6.74 (dd, 1H, J = 8.0, 2.0 Hz, CH), 6.78 (d, 1H, J = 8.0 Hz, CH), 6.84 (s, 2H, 2 × CH), 6.85 (d, 1H, J = 16.0 Hz, CH), 6.88 (d, 1H, J = 2.0 Hz, CH), 7.03 (d, 1H, J = 16.0 Hz, CH) | (CDCl <sub>3</sub> , 101 MHz): δ 153.3, 147.4, 138.4, 136.0, 133.5, 130.3, 128.2, 126.3, 117.8, 112.2, 110.3, 103.2, 60.9, 56.0, 55.5             |
| 9                   | 66        | 127.0–127.5     | 345.35 | (M + Na) <sup>+</sup> 368.1105 | (CDCl <sub>3</sub> , 500 MHz): δ 3.71 (s, 6H, 2 × OCH <sub>3</sub> ), 3.84 (s, 3H, OCH <sub>3</sub> ), 3.93 (s, 3H, OCH <sub>3</sub> ), 6.44 (d, 1H, J = 12.0 Hz, CH), 6.46 (s, 2H, 2 × CH), 6.58 (d, 1H, J = 12.0 Hz, CH), 6.93 (d, 1H, J = 8.0 Hz, CH), 7.42 (dd, 1H, J = 8.0, 2.0 Hz, CH), 7.79 (d, 1H, J = 2.0 Hz, CH)                                 | (CDCl <sub>3</sub> , 75 MHz): δ 153.2, 151.7, 139.5, 137.7, 134.6, 131.8, 131.3, 129.7, 126.9, 125.9, 113.1, 105.8, 61.0, 56.6, 56.9              |
| 10                  | 64        | 159.0–160.0     | 345.35 | (M + Na) <sup>+</sup> 368.1105 | (CDCl <sub>3</sub> , 500 MHz): δ 3.89 (s, 3H, OCH <sub>3</sub> ), 3.92 (s, 6H, 2 × OCH <sub>3</sub> ), 3.99 (s, 3H, OCH <sub>3</sub> ), 6.73 (s, 2H, 2 × CH), 6.93 (d, 1H, J = 16.0 Hz, CH), 7.00 (d, 1H, J = 16.0 Hz, CH), 7.09 (d, 1H, J = 8.0 Hz, CH), 7.65 (dd, 1H, J = 8.0, 2.0 Hz, CH), 8.01 (d, 1H, J = 2.0 Hz, CH)                                 | (CDCl <sub>3</sub> , 75 MHz): δ 153.3, 152.1, 134.6, 133.5, 132.6, 132.3, 131.8, 129.3, 125.1, 123.9, 122.9, 103.6, 63.3, 60.8, 56.5              |
| 11                  | 50        | 101.8–102.4     | 359.37 | (M + H) <sup>+</sup> 360.1438  | (CDCl <sub>3</sub> , 500 MHz): δ 1.46 (t, 3H, J = 5.0 Hz, CH <sub>3</sub> ), 3.72 (s, 6H, 2 × OCH <sub>3</sub> ), 3.85 (s, 3H, OCH <sub>3</sub> ), 4.15 (q, 2H, J = 5.0 Hz, CH <sub>2</sub> ), 6.43–6.47 (m, 3H, 3 × CH), 6.57 (d, 1H, J = 10.0 Hz, CH), 6.92 (d, 1H, J = 10.0 Hz, CH), 7.39–7.41 (m, 1H, CH), 7.77 (s, 1H, CH)                            | (CDCl <sub>3</sub> , 101 MHz): δ 153.2, 151.0, 139.9, 137.7, 134.4, 131.8, 131.2, 129.5, 126.9, 125.8, 114.1, 105.9, 65.5, 61.0, 56.0, 14.5       |
| 12                  | 20        | 132.4–132.9     | 359.37 | (M + H) <sup>+</sup> 360.1438  | (CDCl <sub>3</sub> , 500 MHz): δ 1.49 (t, 3H, J = 5.0 Hz, CH <sub>3</sub> ), 3.88 (s, 3H, OCH <sub>3</sub> ), 3.92 (s, 6H, 2 × OCH <sub>3</sub> ), 4.21 (q, 2H, J = 5.0 Hz, CH <sub>2</sub> ), 6.73 (s, 2H, 2 × CH), 6.93 (d, 1H, J = 15.0 Hz, CH), 6.99 (d, 1H, J = 15.0 Hz, CH), 7.06 (d, 1H, J = 10.0 Hz, CH), 7.61–7.63 (m, 1H, CH), 7.97 (s, 1H, CH)  | (CDCl <sub>3</sub> , 101 MHz): δ 153.5, 151.5, 140.2, 138.3, 132.4, 131.6, 130.1, 129.4, 125.3, 122.9, 114.8, 103.7, 65.6, 61.0, 56.2, 14.6       |

<sup>a</sup>nd, not determined.

group in part C was replaced by an ethoxy group to afford 12 combretastatin A-4 derivatives, respectively (Figure 1). The synthesis of the derivatives is outlined in Figure 2 with the methods previously reported.<sup>9</sup> All of the structure elucidation data are presented in Table 1. *E*-Diphenylethene and *Z*-diphenylethene were characterized by the different <sup>1</sup>H NMR coupling constants. The *J* values of 8 (*E*-diphenylethene) and 7 (*Z*-diphenylethene) are 16.0 and 12.0 Hz, respectively.

**Table 2. Antifungal Activities of Combretastatin A-4 and Derivatives**

| compound            | EC <sub>50</sub> value (μM) |                  | inhibition at 50 μg/mL <sup>a</sup> (%) |                     |
|---------------------|-----------------------------|------------------|---|---------------------|
|                     | <i>R. solani</i>            | <i>P. oryzae</i> | <i>S. sclerotio</i>                     | <i>F. oxysporum</i> |
| combretastatin A-4  | 46.5                        | 104              | 27.7                                    | 53.3                |
| combretastatin A-4P | no effect                   | no effect        | -0.6                                    | 17.2                |
| 1                   | 75.6                        | 271              | -1.5                                    | 15.1                |
| 2                   | 51.6                        | 99.6             | 24.7                                    | 31.9                |
| 3                   | 355                         | 383              | 0.3                                     | 16.7                |
| 4                   | 238                         | 369              | 4.9                                     | 21.9                |
| 5                   | no effect                   | no effect        | -1.2                                    | 29.2                |
| 6                   | no effect                   | no effect        | -0.6                                    | 27.4                |
| 7                   | 94.0                        | 159              | 11.6                                    | 36.6                |
| 8                   | no effect                   | no effect        | -1.5                                    | 16.4                |
| 9                   | 261                         | 624              | 0.9                                     | 15.1                |
| 10                  | no effect                   | no effect        | -3.7                                    | 12.0                |
| 11                  | 188                         | 291              | 4.9                                     | 24.0                |
| 12                  | no effect                   | no effect        | -0.9                                    | 14.4                |
| carbendazim         | - <sup>b</sup>              | -                | 5.8                                     | 21.7                |
| isoprothiolane      | 64.5                        | 324              | -                                       | -                   |

<sup>a</sup>Inhibition against carbendazim resistance strains. <sup>b</sup>-, not tested.

**Biological Evaluations and SAR Assay.** The antifungal effects of combretastatin A-4, combretastatin A-4P, and derivatives were determined from concentration–response curves with rice sheath blight disease (*R. solani*) and rice blast disease (*P. oryzae*) as the tested strains. The EC<sub>50</sub> value of each compound is shown in Table 2. As isoprothiolane is a commercial fungicide widely used for rice disease control, it was selected as a positive control in our experiment. For the rice sheath blight disease control, combretastatin A-4 and 2 showed significant effects, with EC<sub>50</sub> values of 46.5 and 51.6 μM, respectively, compared with isoprothiolane (EC<sub>50</sub> value = 64.5 μM). Combretastatin A-4, 1, 2, 7, and 11 were more active than isoprothiolane in the antifungal assay against *P. oryzae*.

The double bond in part A of combretastatin A-4 was hydrogenated to afford the final product. The antifungal effects of 1 and combretastatin A-4 are similar, which suggested that the single bond retains the antifungal activity. It is obvious that the effect is completely lost when the natural *cis* configuration is transformed to the *trans* configuration. Structural modifications to the hydroxyl group in part B indicate that the amino group maintained the activity; however, the nitro and disodium phosphate groups completely eliminated the antifungal activity. The bioassay results for compounds 2 and 4 indicated that the introduction of an ethoxy group replacing the methoxy group in part C enhanced bioactivity against the rice diseases.

**Molecular Modeling.** Molecular modeling studies were undertaken to determine the interaction between combretastatin A-4 and fungal tubulin. The studies were performed with homology modeling and the Surflex-Dock module in the Sybyl program. The homology model of β-tubulin of *R. solani*

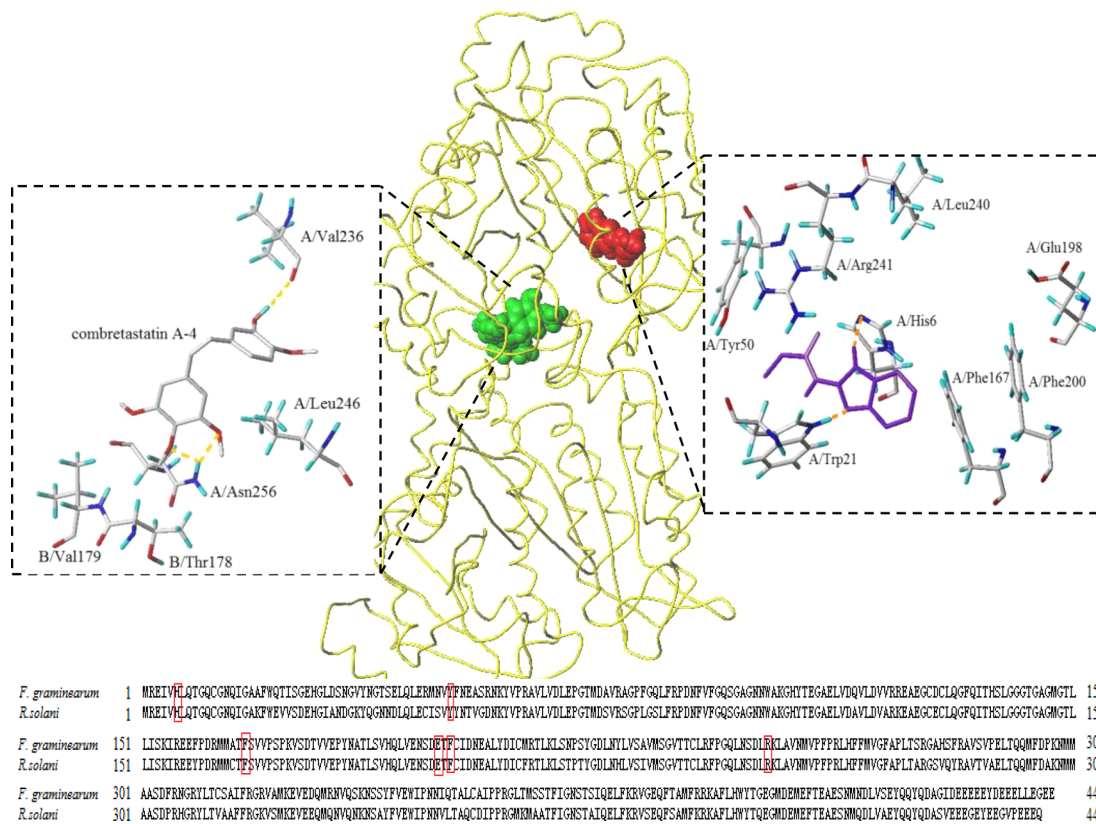


**Figure 3.** Binding sites of combretastatin A-4 and carbendazim in *R. solani* β-tubulin. Combretastatin A-4 is shown with green spacefill and carbendazim with red spacefill. Hydrogen bonds are shown with dotted yellow lines. The conserved amino acid residues are highlighted in a red box.

(GenBank CUA76508.1) was generated with the crystal structure of cow's brain  $\beta$ -tubulin (PDB ID 1Z2Bb) as the template. A sequence alignment showed their sequence identity value was 86%. Combretastatin A-4 and carbendazim were used to identify the receptor binding pockets and to analyze the binding characteristics with a blind docking calculation in this study. The colchicine binding site of tubulin has been validated as the binding pocket of combretastatin A-4 (Figure 3) between two adjacent subunits of tubulin.<sup>16</sup> Thus, the colchicine binding site was used for the docking simulation of combretastatin A-4 and derivatives. Hydrogen-bonding interactions show that combretastatin A-4 is bound to Val236 and Asn256 of subunit A of the  $\beta$ -tubulin model. This suggested a hydrogen-bonding interaction between the hydroxyl group of combretastatin A-4 and Val236 is critical for full biological activity, which explains why the biological activity was lost if the hydroxyl group was replaced by a nitro or disodium phosphate group. Figure 2 shows that the carbendazim binding site is different from that of combretastatin A-4. Carbendazim has interactions only with one subunit of  $\beta$ -tubulin. Qiu et al.<sup>17</sup> demonstrated the possible binding pocket for carbendazim on the  $\beta_2$ -tubulin in *Gibberella zeae* was formed with residues Tyr50, Phe167, Glu198, Phe200, and Arg241. Sequence alignment showed those above residues are conserved (Figure 3). The carbendazim binding pocket of *R. solani*  $\beta$ -tubulin was also formed with those residues. In addition, His6 and Trp21 formed two hydrogen bonds with carbendazim in our model, explaining why mutations at the codons 6 gene were responsible for resistance to carbendazim.<sup>7</sup>

It is obvious that the binding sites of combretastatin A-4 and carbendazim on fungal tubulin are totally different, which suggested that combretastatin A-4 and derivatives can be the useful for controlling carbendazim-resistant plant diseases.

**Antifungal Effects on Resistant Strains.** Two carbendazim-resistant strains (*Fusarium oxysporum* Schl. f. sp. *vasinfectum* (Atk.) Snyder & Hans and *Sclerotinia sclerotiorum* (Lib.) de Bary) were used to test the antifungal effects of combretastatin A-4 and derivatives on the resistant fungi. The results demonstrated that combretastatin A-4 and **2** have appreciable inhibitory ability to the resistant fungi, compared with carbendazim (Table 2). On testing with *F. oxysporum*, the inhibition by combretastatin A-4 was 2.5-fold greater than that of carbendazim. Combretastatin A-4 and **2** have nearly 5- and 4-fold more antifungal effects than carbendazim against *S. sclerotiorum*. This result showed that the binding sites of combretastatin A-4 and derivatives are different from that of carbendazim, which suggested that combretastatin A-4 is a good lead compound for new fungicide discovery that can be used for the control of carbendazim-resistant fungi.

In conclusion, combretastatin A-4 was first isolated from the African willow tree, and the double bond in part A of combretastatin A-4 was hydrogenated; the hydroxyl group in part B was replaced by amino, nitro, or disodium phosphate group, and the methoxy group in part C was replaced by an ethoxy group to afford 12 combretastatin A-4 derivatives, respectively. Combretastatin A-4 and its derivatives were identified as new potential fungicides targeting fungal tubulin. Because their binding site is entirely different from that of carbendazim, they are possibly useful for fungal resistance management. The results of antifungal assays on resistant strains confirmed our hypothesis.

## AUTHOR INFORMATION

### Corresponding Authors

\* (Z.-P.K.) Phone: +86 136 71951027. Fax: +86 21 60877220. E-mail: kaizp@sit.edu.cn.

\* (F.-H.W.) Phone: +86 21 60877220. Fax: +86 21 60877220. Email: wfh@sit.edu.cn.

### Funding

This work was supported by grants from the National Natural Science Foundation of China (No. 21402122 and 21472126). It was also supported by the Natural Science Foundation of Shanghai (No. 14ZR1440600) and the Innovation Program of Shanghai Municipal Education Commission (No. 14YZ148).

### Notes

The authors declare no competing financial interest.

## REFERENCES

- (1) Pettit, G. R.; Singh, S. B.; Hamel, E.; Lin, C. M.; Alberts, D. S.; Kendall, D. G. Isolation and structure of the strong cell growth and tubulin inhibitor combretastatin A-4. *Experientia* **1989**, *45*, 209–211.
- (2) Salehi, M.; Ostad, S. N.; Riazi, G. H.; Assadieskandar, A.; Shavi, T. C.; Shafiee, A.; Amini, M. Synthesis, cytotoxic evaluation, and molecular docking study of 4,5-diaryl-thiazole-2-thione analogs of combretastatin A-4 as microtubule-binding agents. *Med. Chem. Res.* **2014**, *23*, 1465–1473.
- (3) Hamze, A.; Rasolofonjatovo, E.; Provot, O.; Mousset, C.; Veau, D.; Rodrigo, J.; Bignon, J.; Liu, J. M.; Bakala, J. W.; Thoret, S.; Dubois, J.; Brion, J. D.; Alami, M. B-Ring-Modified isoCombretastatin A-4 analogues endowed with interesting anticancer activities. *ChemMedChem* **2011**, *6*, 2179–2191.
- (4) Qin, Y. J.; Li, Y. J.; Jiang, A. Q.; Yang, M. R.; Zhu, Q. Z.; Dong, H.; Zhu, H. L. Design, synthesis and biological evaluation of novel pyrazoline-containing derivatives as potential tubulin assembling inhibitors. *Eur. J. Med. Chem.* **2015**, *94*, 447–457.
- (5) Verhey, K. J.; Gaertig, J. The tubulin code. *Cell Cycle* **2007**, *6*, 2152–2160.
- (6) Bollen, G. J.; Scholten, G. Acquired resistance to benomyl and some other systemic fungicides in a strain of *Botrytis cinerea* in cyclamen. *Neth. J. Plant Pathol.* **1971**, *77*, 83–90.
- (7) Qiu, J. B.; Huang, T. T.; Xu, J. Q.; Bi, C. W.; Chen, C. J.; Zhou, M. G.  $\beta$ -Tubulins in *Gibberella zeae*: their characterization and contribution to carbendazim resistance. *Pest Manage. Sci.* **2012**, *68*, 1191–1198.
- (8) Shen, W. P.; Diao, Y. J.; Jin, H. M.; Wang, J. P.; Wang, J. G. Synthesis of combretastatin A-4 supported by polymer. Chinese Patent CN 1704393A, 2005.
- (9) Zhao, L.; Zhou, J. J.; Huang, X. Y.; Cheng, L. P.; Pang, W.; Kai, Z. P.; Wu, F. H. Design, synthesis and anti-proliferative effects in tumor cells of new combretastatin A-4 analogs. *Chin. Chem. Lett.* **2015**, *26*, 993–999.
- (10) Shi, J.; Blundell, T. L.; Mizuguchi, K. FUGUE: sequence-structure homology recognition using environment-specific substitution tables and structure-dependent gap penalties. *J. Mol. Biol.* **2001**, *310*, 243–257.
- (11) Sutcliffe, M. J.; Haneef, I.; Carney, D.; Blundell, T. L. Knowledge based modelling of homologous proteins, part I: three-dimensional frameworks derived from the simultaneous superposition of multiple structures. *Protein Eng., Des. Sel.* **1987**, *1*, 377–384.
- (12) Halgren, T. A. MMFF VI. MMFF94s option for energy minimization studies. *J. Comput. Chem.* **1999**, *20*, 720–729.
- (13) Head, J. D.; Zerner, M. C. A Broyden-Fletcher-Goldfarb-Shanno optimization procedure for molecular geometries. *Chem. Phys. Lett.* **1985**, *122*, 264–270.
- (14) Kai, Z. P.; Ling, Y.; Liu, W. J.; Zhao, F.; Yang, X. L. The study of solution conformation of allatostatins by 2-D NMR and molecular modeling. *Biochim. Biophys. Acta, Proteins Proteomics* **2006**, *1764*, 70–75.

- (15) Spitzer, R.; Jain, A. N. Surflex-Dock: docking benchmarks and real-world application. *J. Comput.-Aided Mol. Des.* **2012**, *26*, 687–699.
- (16) Chen, J.; Liu, T.; Dong, X.; Hu, Y. Z. Recent development and SAR analysis of colchicine binding site inhibitors. *Mini-Rev. Med. Chem.* **2009**, *9*, 1174–1190.
- (17) Qiu, J. B.; Xu, J. Q.; Yu, J. J.; Bi, C. W.; Chen, C. J.; Zhou, M. G. Localisation of the benzimidazole fungicide binding site of *Gibberella zeae*  $\beta_2$ -tubulin studied by site-directed mutagenesis. *Pest Manage. Sci.* **2011**, *67*, 191–198.